Supplementary Information (SI) for Nanoscale.
This journal is © The Royal Society of Chemistry 2026

# Supporting Information

## A hierarchical 3D Fe-doped $Bi_2MoO_6$ arrays supported on Ni-Foam: An effective electrocatalyst for alkaline water splitting

**Dinesh Singh[†,‡], Pankaj Poddar[†,‡,*]**

[†]*Physical & Materials Chemistry Division, CSIR-National Chemical Laboratory, Pune 411008, India*
[‡]*Academy of Scientific and Innovative Research (AcSIR), Sector 19, Kamla Nehru Nagar, Ghaziabad, Uttar Pradesh- 201002, India*
*Corresponding author e-mail: p.poddar@ncl.res.in.

## 2.3 Material characterization

### 2.3.1 Characterisation techniques

The samples' X-ray diffraction patterns were obtained with a Smartlab X-ray diffraction (Rigaku) instrument. The diffraction angle 2θ was scanned from 10˚ to 80˚ using Cu Kα radiation filtered with iron (λ = 1.54 Å) and a step size of 0.01˚. The FESEM (Hitachi S-4200) was employed for morphological analysis. The FEI Tecnai T20 High-Resolution Transmission Electron Microscopy (HRTEM) was utilised to analyse the morphology, particle size, and d-spacing at an accelerating voltage of 200 keV. The XPS was used to record the X-ray photoelectron spectra of Bi, Mo, O, and Fe. The experiment utilised a monochromatic X-ray source with Al Kα radiation (hv = 1486.6 eV) operating at 6 mA and 12 kV, coupled with a Physical Electronics 04-548 dual Mg/Al anode. The system was maintained under ultra-high vacuum conditions with a base pressure of $\leq 5 * 10^{-9}$ Torr. A spot size of 400 μm was utilised in the XPS measurement. XPS peak 4.123 software was used to deconvolute the recorded data. The XPS measurement was performed by cutting the deposited Ni-foam (10 mm X 10 mm piece) and then using a surface etching process to minimise the possibility of contaminants on the surface. The electron paramagnetic resonance (EPR) spectra were recorded at room temperature using a Bruker EMX Plus spectrometer. Raman spectra were acquired using an IndiRAM CTR-500C Raman spectrometer equipped with a 532 nm excitation laser.

### 2.3.2 Electrocatalytic measurements

All the OER and HER performances were measured using a CHI600E potentiostat, where the nickel foam (area = 1 cm × 1 cm), Hg/HgO, and graphite rod were used as working, reference, and counter electrodes, respectively. The potential has been calibrated against the reversible hydrogen electrode (RHE) with the iR-corrected polarisation curve using the following equation.

$$E_{RHE} = E_{Hg/HgO} + 0.0591pH + 0.098 \quad (1)$$

All electrochemical measurements were performed in 1.0 M KOH solution (pH ~13.6). Before the OER and HER performance test, the working electrode was stabilized by cyclic voltammetry (CV) scans at 100 mV/s for several cycles. The linear sweep voltammetry (LSV) scans were carried out at a 5 mV/s scan rate with 90 % iR compensation (during running the LSV scan) to remove the

electrolyte solution resistance. The electrocatalytic stability of the as-synthesized electrocatalyst was measured by chronopotentiometry by applying the constant current density of 10 mA/cm$^2$ for 22 h for OER and 24 h for HER. Electrochemically active surface area (ECSA) is utilised to learn the properties of the catalyst's surface and how they reflect the catalyst's intrinsic activity. The following calculation, based on the ECSA's relationship to the double-layer capacitance, can be used to get the actual ECSA value ($C_{dl}$):

ECSA = $C_{dl}/C_s$

$C_s$ is the specific capacitance of a 1 cm$^2$ standard electrode. $C_s$ for nickel foam electrodes on a flat surface is typically 40 μF cm$^{-2}$, but can range from 20 to 60 μF cm$^{-2}$. In this case, the double-layer capacitance (Cdl) was determined by plotting the linear relationship between the capacitive current (ic) and the scan rate, as obtained from cyclic voltammetry (CV) measurements performed in the non-Faradaic region. For the BMO sample, the potential window was selected between 1.105 and 1.205 V, whereas for the BMOF-5 sample, the CV scan was carried out within the potential range of 1.045–1.145 V. Here, the CV scans were taken at 20, 40, 60, 80, and 100 mV/s scan rate. The EIS (Electrochemical Impedance Spectroscopy) data were recorded between 0.1 Hz and 100 kHz frequency at 0.65 VvsHg/HgO or 1.575 VvsRHE potential for OER and -1.10 $V_{vs}$Hg/HgO or -0.175 $V_{vs}$RHE potential for HER.

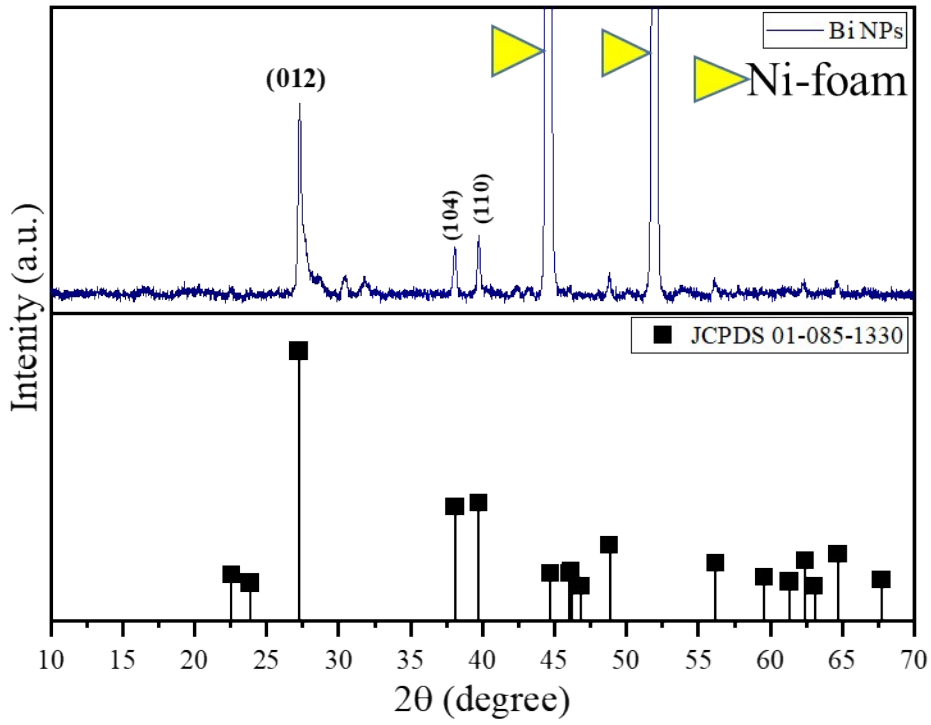


**Figure S1:** High glycerol (95% by volume) content during the synthesis process facilitates the formation of Bismuth nanoparticles.

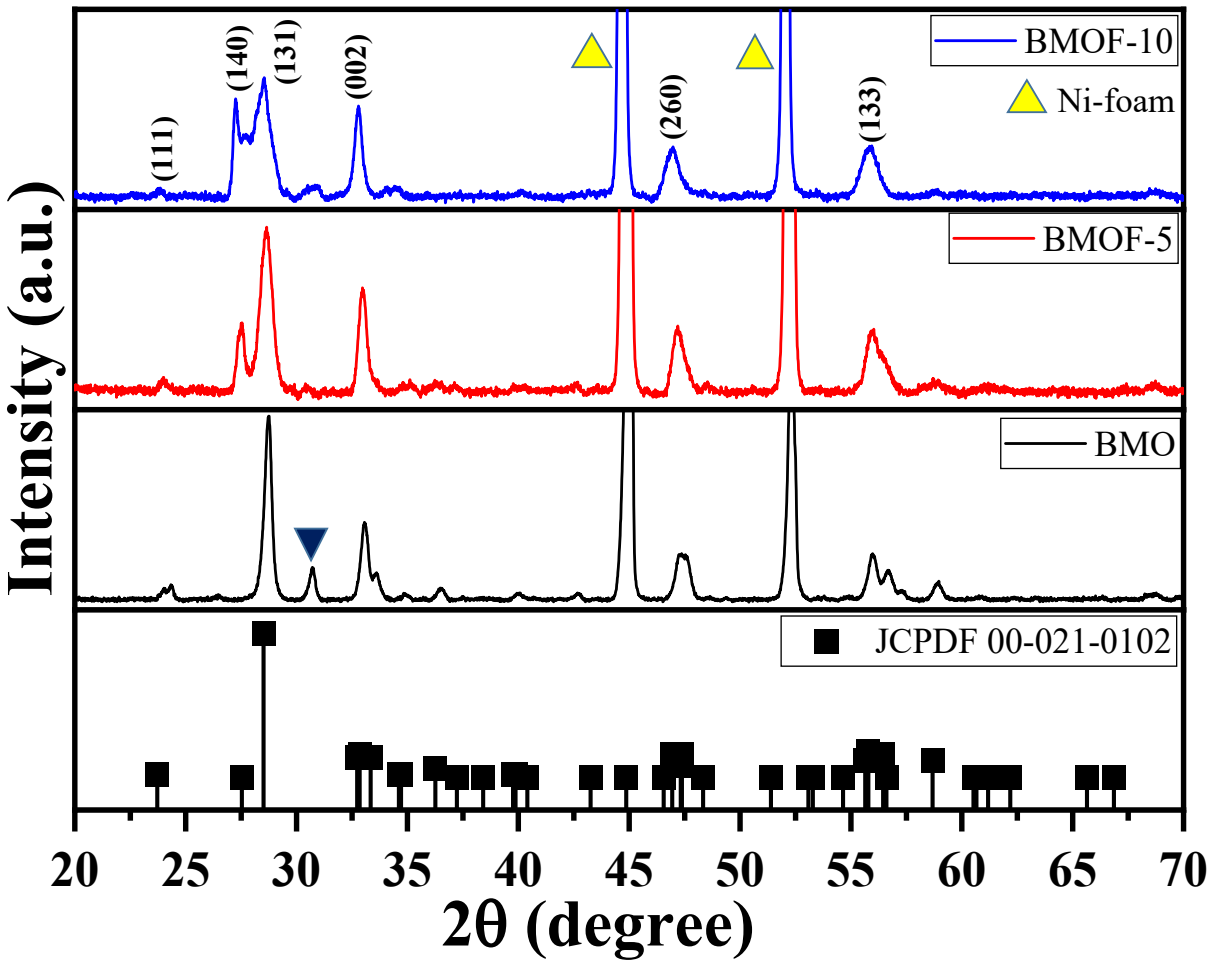


**Figure S2:** Zoom in view of PXRD patterns on the nickel foam substrate with their standard JCPDS file.

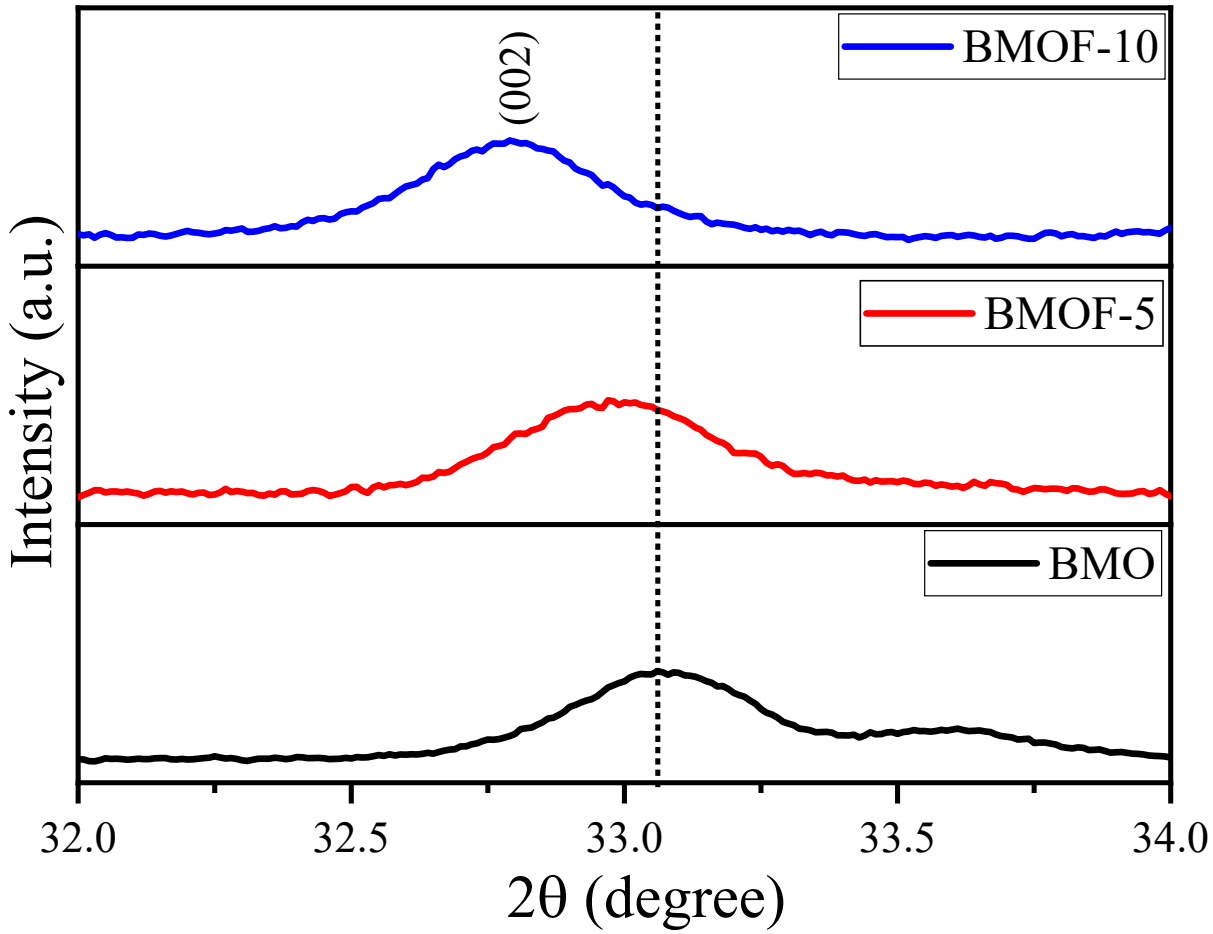


**Figure S3:** Shift in (002) peak, BMOF-5 and BMOF-10 from BMO after partial substitution of bismuth ions with iron ions.

| **Samples** | **Crystallite size with respect to the (131) lattice plane** | **Crystallite size with respect to the (002) lattice plane** | **Average crystallite size with respect to (131) and (002)** |
|---|---|---|---|
| BMO | 25 ± 4 | 22 ± 4 | 23 ± 4 |
| BMOF-5 | 17 ± 4 | 21 ± 4 | 19 ± 4 |
| BMOF-10 | 12 ± 4 | 20 ± 4 | 16 ± 4 |

**Table S1:** Average crystallite size with respect to (131) and (002) lattice plane.

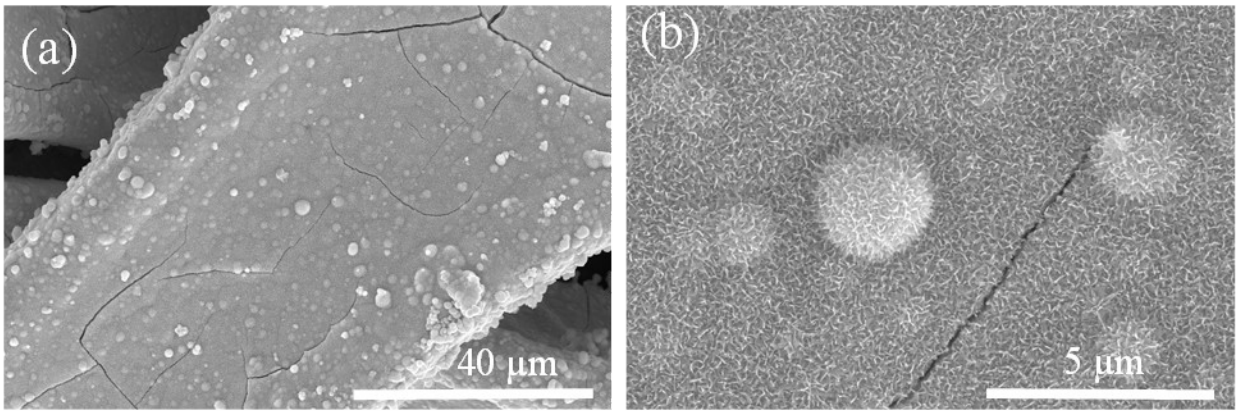


**Figure S4:** FESEM Morphology of (a, b) BMO sample at 40 µm and 5µm scales.

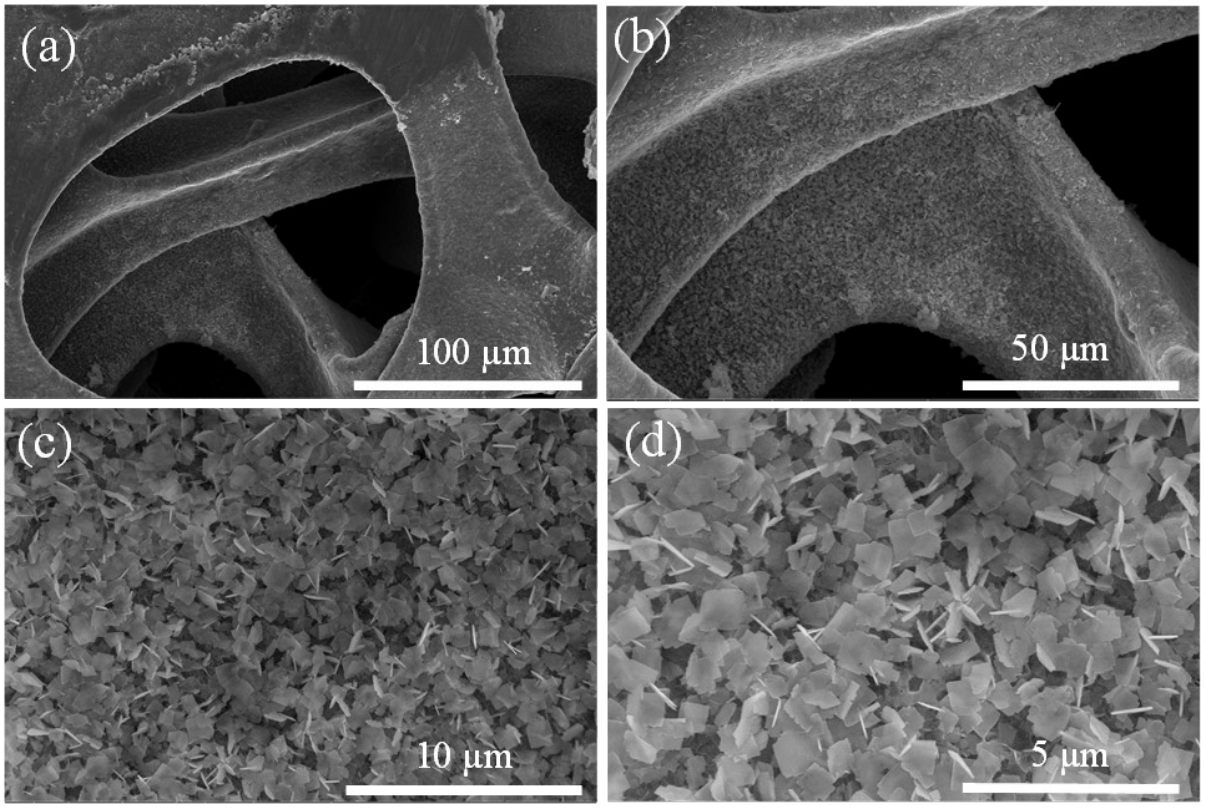


**Figure S5:** Morphology (FESEM images) of BMOF-10 (a, b, c, and d) sample at various scales.

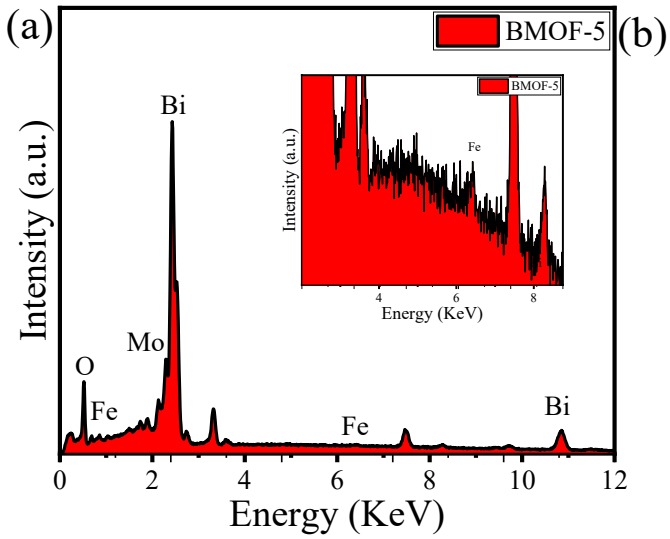


(b)

| Elements | Weight % |
|---|---|
| O K | 16 ± 1 |
| MoL | 15 ± 1 |
| BiM | 64 ± 1 |
| FeK | 5 ± 1 |

**Figure S6:** (a) EDAX spectrum of BMOF-5, figure inset zoom view (b) weight percentage of BMOF-5.

| **Samples** | **Iron (Fe) Weight (%)** |
|---|---|
| BMO | 0 |
| BMOF-5 | 4 ± 1 |
| BMOF-10 | 9 ± 1 |

**Table S2:** ICP-OES results for iron.

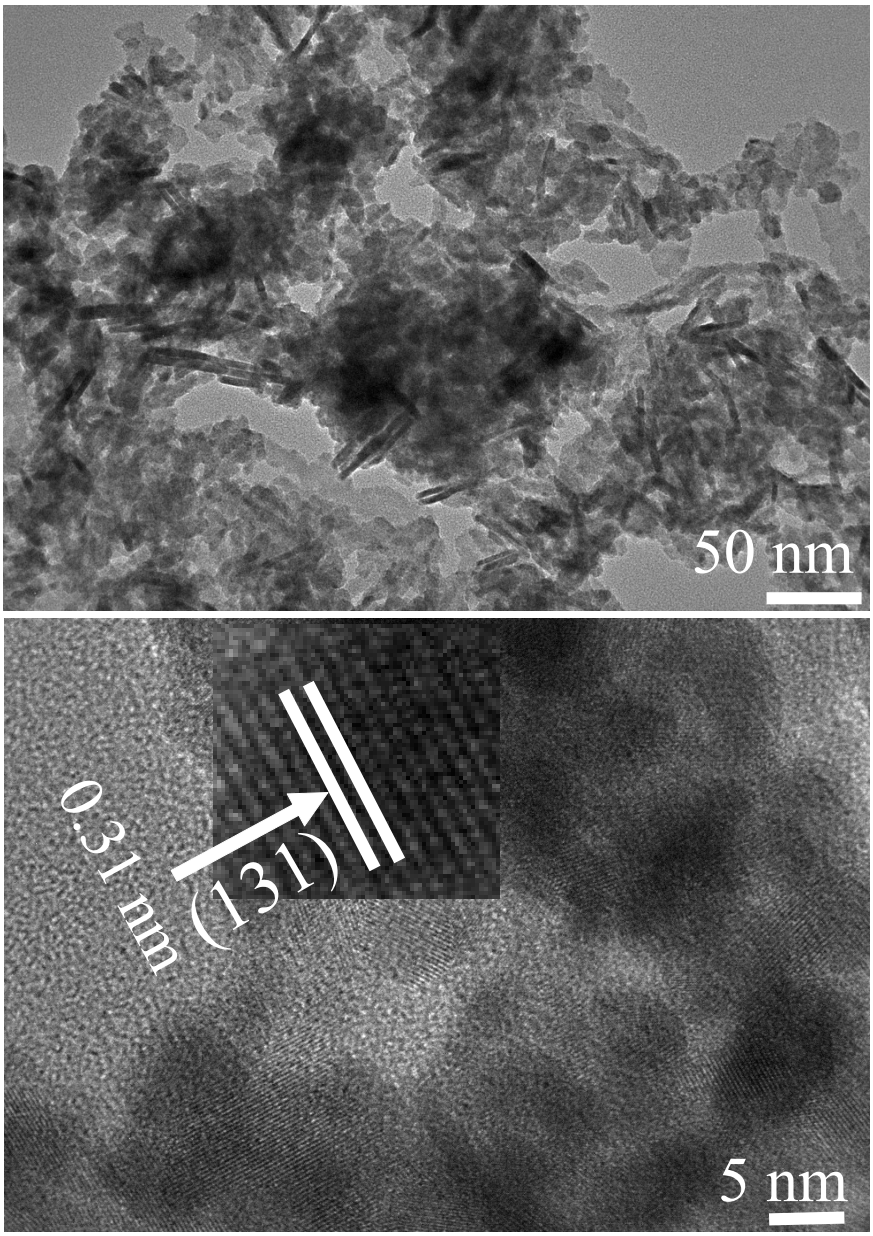


**Figure S7:** (a) TEM image at 50 nm scale, and (b) d-spacing between 131 lattice planes of the BMO sample.

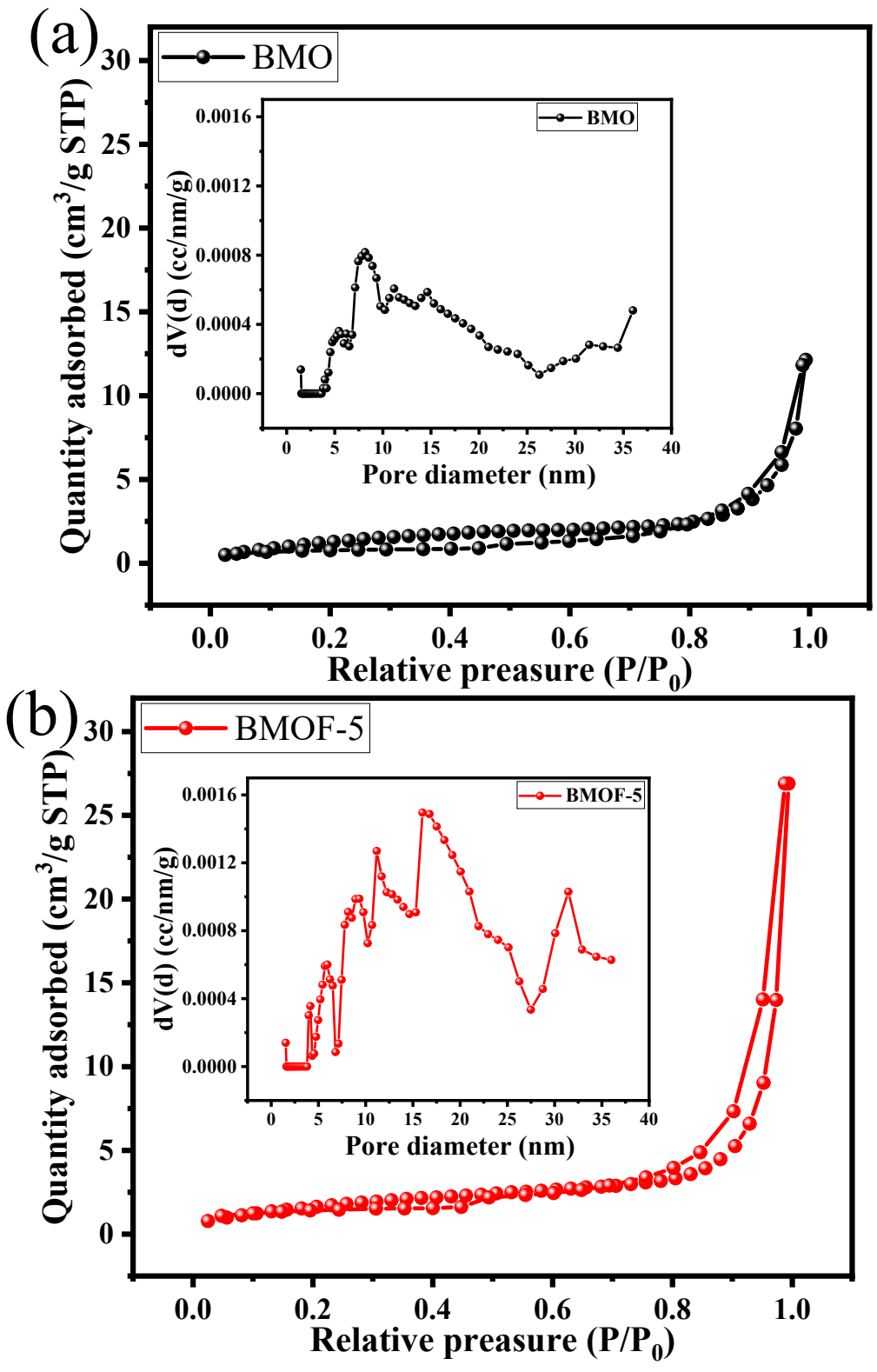


**Figure S8:** BET surface area of (a) BMO and (b) BMOF-5 samples. Figure inset pore diameter.

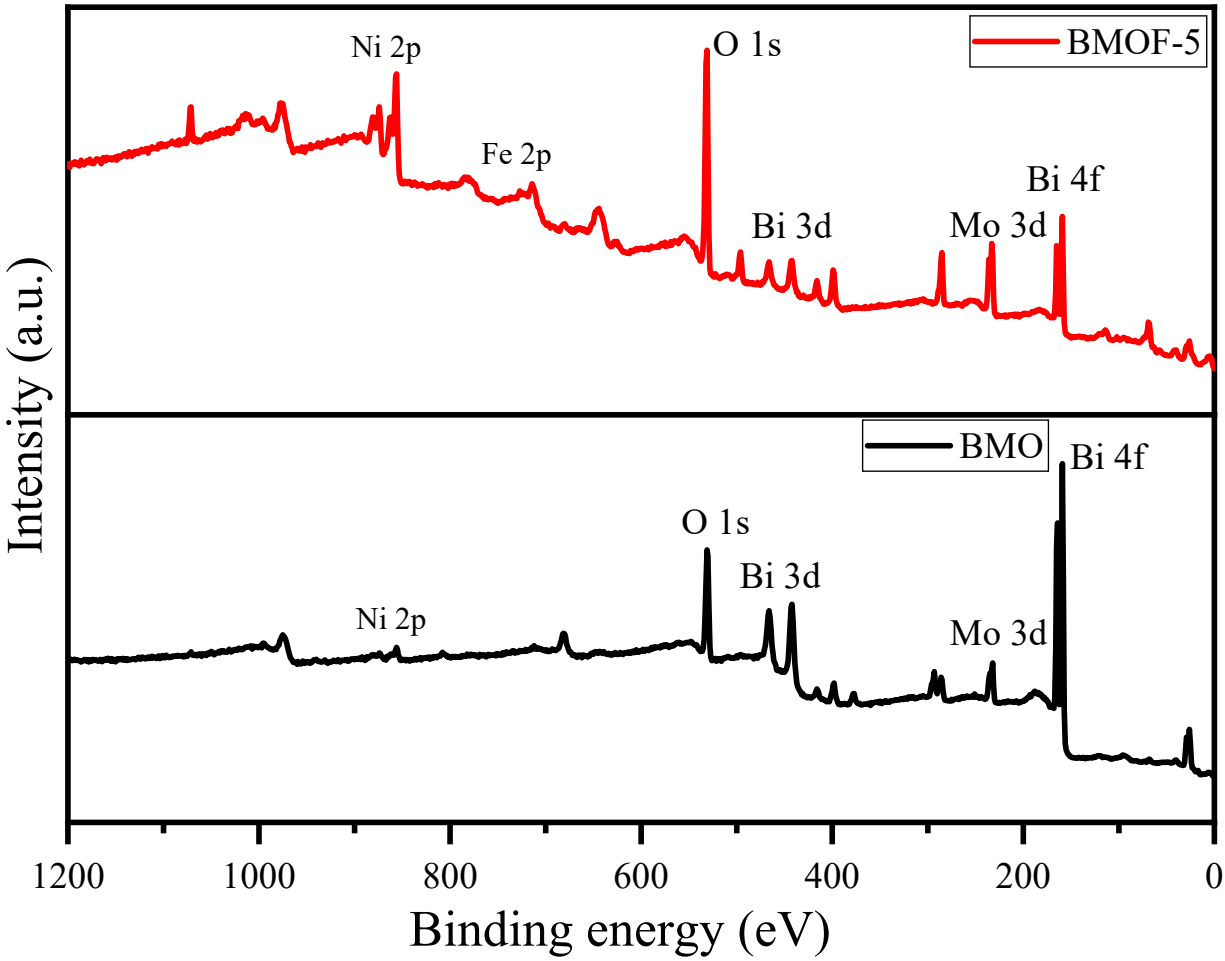


**Figure S9:** Survey spectrum of BMO and BMOF-5.

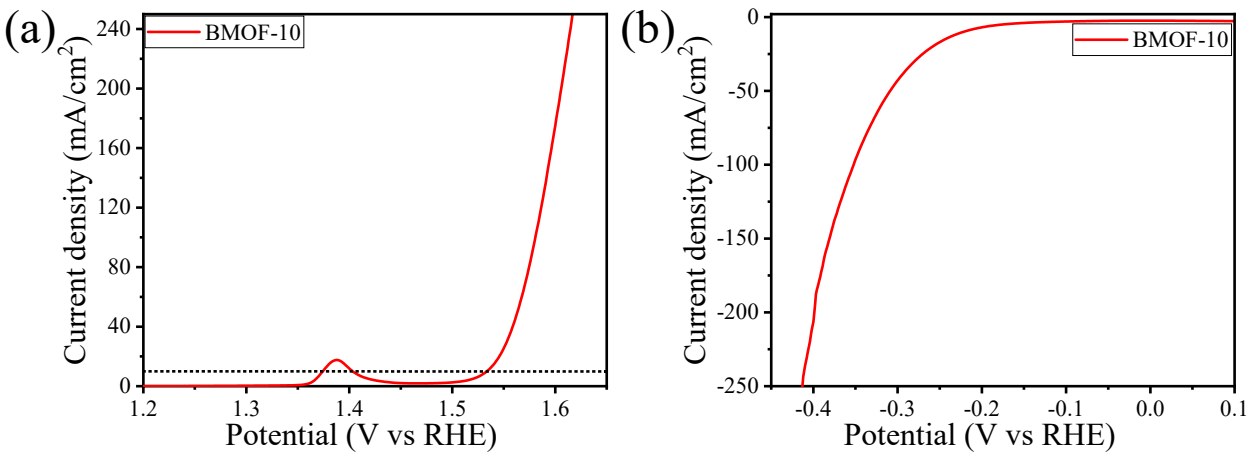


**Figure S10:** Electroctalytic (a) OER and (b) HER LSV plot of sample BMOF-10.

| S.No. | Catalyst | Substrate | Method | Electrolyte | Overpotential (mV) | Current density ($mA/cm^2$) | References |
|---|---|---|---|---|---|---|---|
| 1 | BiOCl/Fe | Ni-foam | Slurry coating | 1 M KOH | 370 | 10 | https://doi.org/10.1021/acs.langmuir.3c01272 |
| 2 | $Bi_2MoO_6$ /Fe | Ni-foam | Slurry coating | 1 M KOH | 286 | 10 | https://doi.org/10.1016/j.cej.2021.131884 |
| 3 | NiOx/Ni | Ni-foam | Electrode position | 1 M KOH | 390 | 10 | https://doi.org/10.1016/j.apsusc.2015.10.097 |
| 4 | Ni@NF | Ni-foam | CVD | 1 M KOH | 285 | 10 | https://doi.org/10.1016/j.ijhydene.2023.01.083 |
| 5 | $Bi_2MoO_6$ /Fe | Ni-foam | In situ hydrothermal | 1 M KOH | 261 | 10 | This work |

**Table S3:** Comparison of OER BMOF-5 electrocatalyst with reported electrocatalyst.

| Samples (OER) | $R_s$ (ohm) | $R_{ct}$ (ohm) |
|---|---|---|
| BMO | 1.45 | 22 |
| BMOF-5 | 1.3 | 2.5 |
| Ni-foam | 1.35 | 45 |

**Table S4:** $R_s$ (solution resistance), and $R_{ct}$ (charge transfer resistance) for OER.

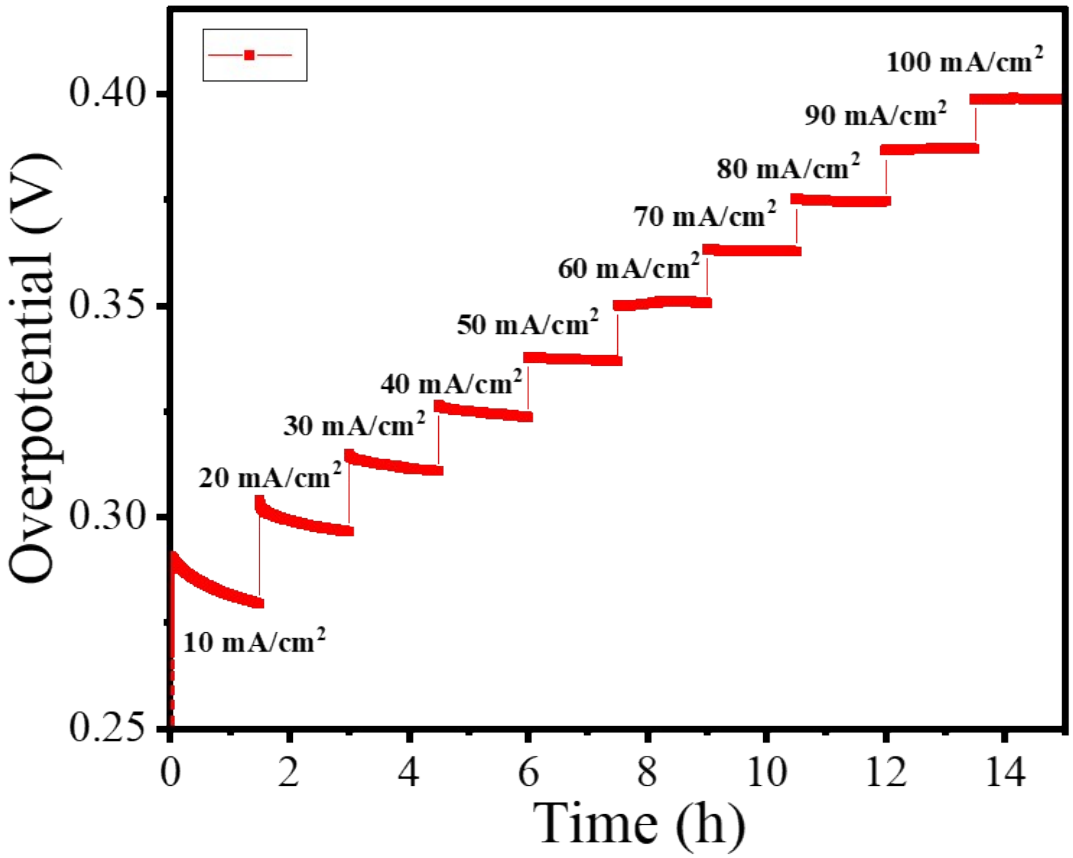


**Figure S11:** Multi-step chronopotentiometry test without iR correction of BMOF-5 phase at 10–100 mA/cm$^2$ current densities.

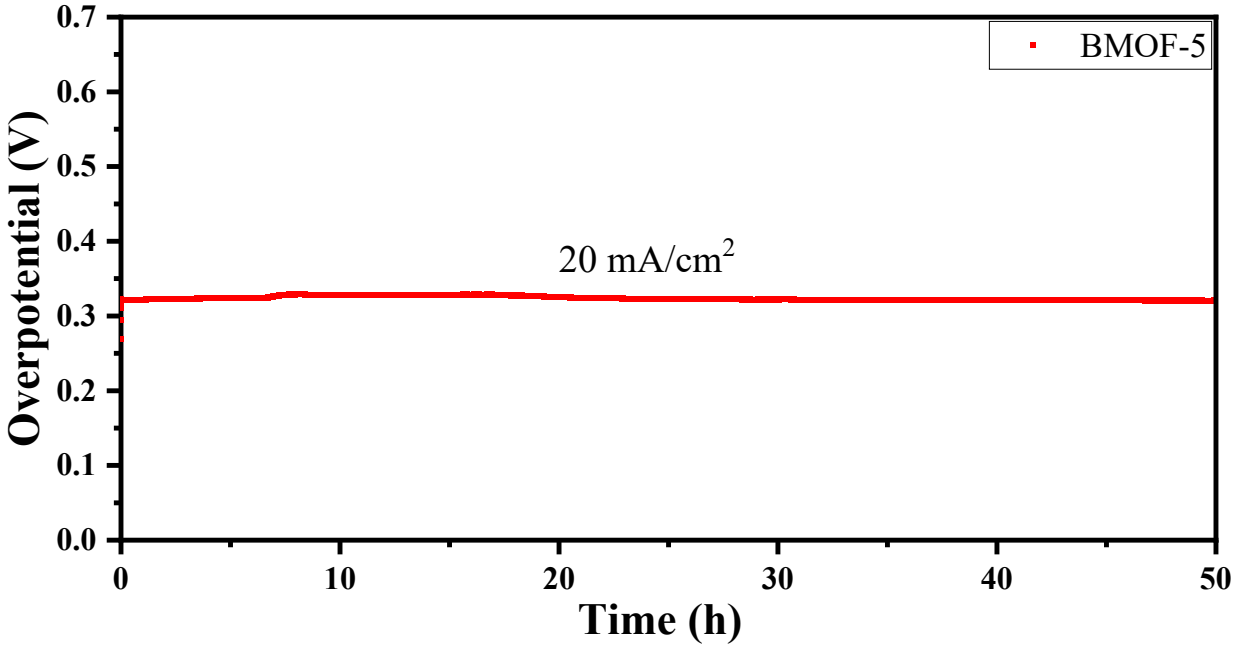


**Figure S12:** Chronopotentiometry test for OER at 20 mA/cm$^2$ current density (without iR correction) of the BMOF-5 sample for 50 h.

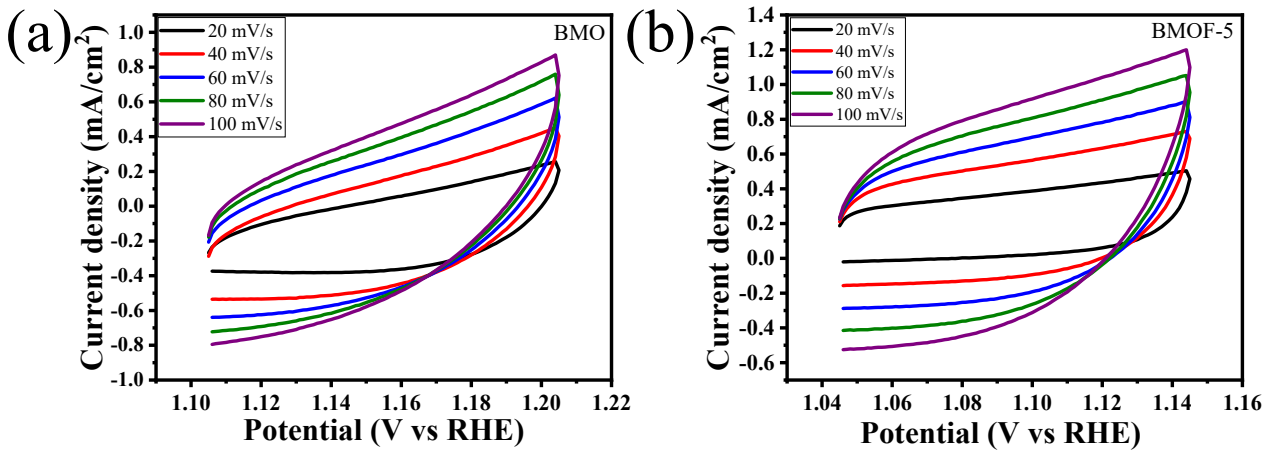


**Figure S13:** Different CV scans at 20, 40, 60, 80, 100 mV (a) BMO, and (b) BMOF-5

| S.No. | Catalyst | Substrate | Electrolyte | Overpotential (mV) | Current density ($mA/cm^2$) | References |
|---|---|---|---|---|---|---|
| 1 | $NiF_2$ | Ni-foam | 1 M KOH | 172 | 10 | https://doi.org/10.1039/D1DT00654A |
| 2 | $NiCo_2S_4$ NW | Ni-foam | 1 M KOH | 260 | 10 | https://doi.org/10.1002/adfm.201600566 |
| 3 | $Ni_3S_2$/NF-4 | Ni-foam | 1 M KOH | 89 | 10 | https://doi.org/10.1021/acsami.8b09361 |
| 4 | $Bi_2S_3$ | Ni-foam | 1 M KOH | 192 | 10 | https://doi.org/10.1016/j.est.2024.112323 |
| 5 | $Bi_2MoO_6$ /Fe | Ni-foam | 1 M KOH | 152 | 10 | This work |

**Table S5:** Comparison of HER electrocatalyst with reported catalyst.

| Samples (HER) | $R_s$ (ohm) | $R_{ct}$ (ohm) |
|---|---|---|
| BMO | 1.72 | 21 |
| BMOF-5 | 1.7 | 8 |
| Ni-foam | 1.71 | 51 |

**Table S6:** $R_s$ and $R_{ct}$ values of HER

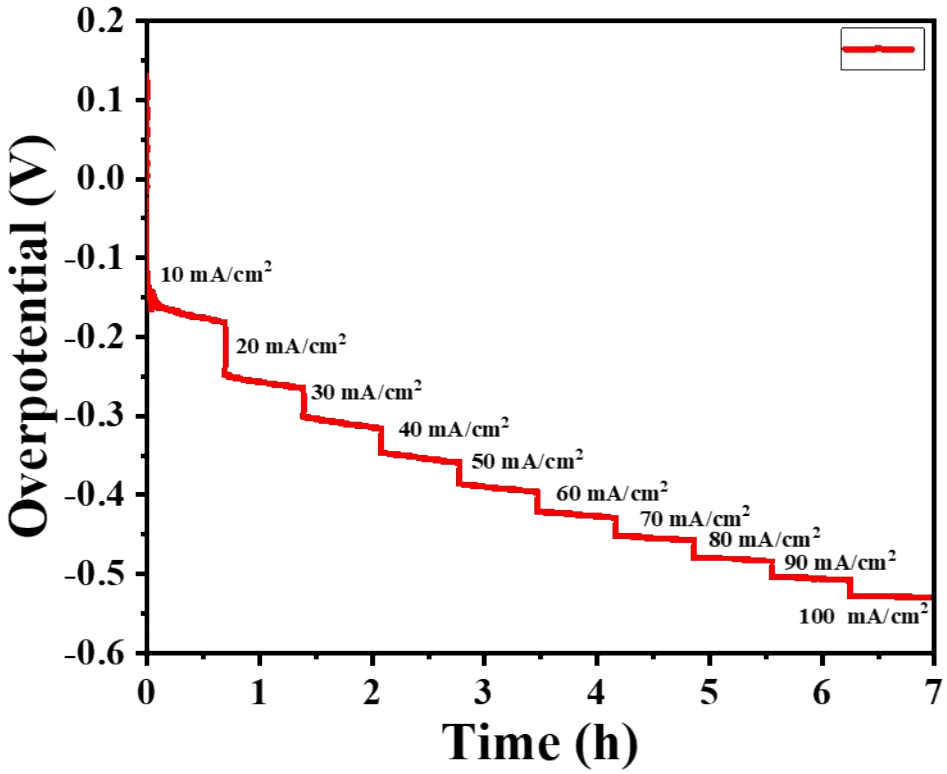


**Figure S14:** Multi-current chronopotentiometry test for HER (without iR correction) of the BMOF-5 sample.

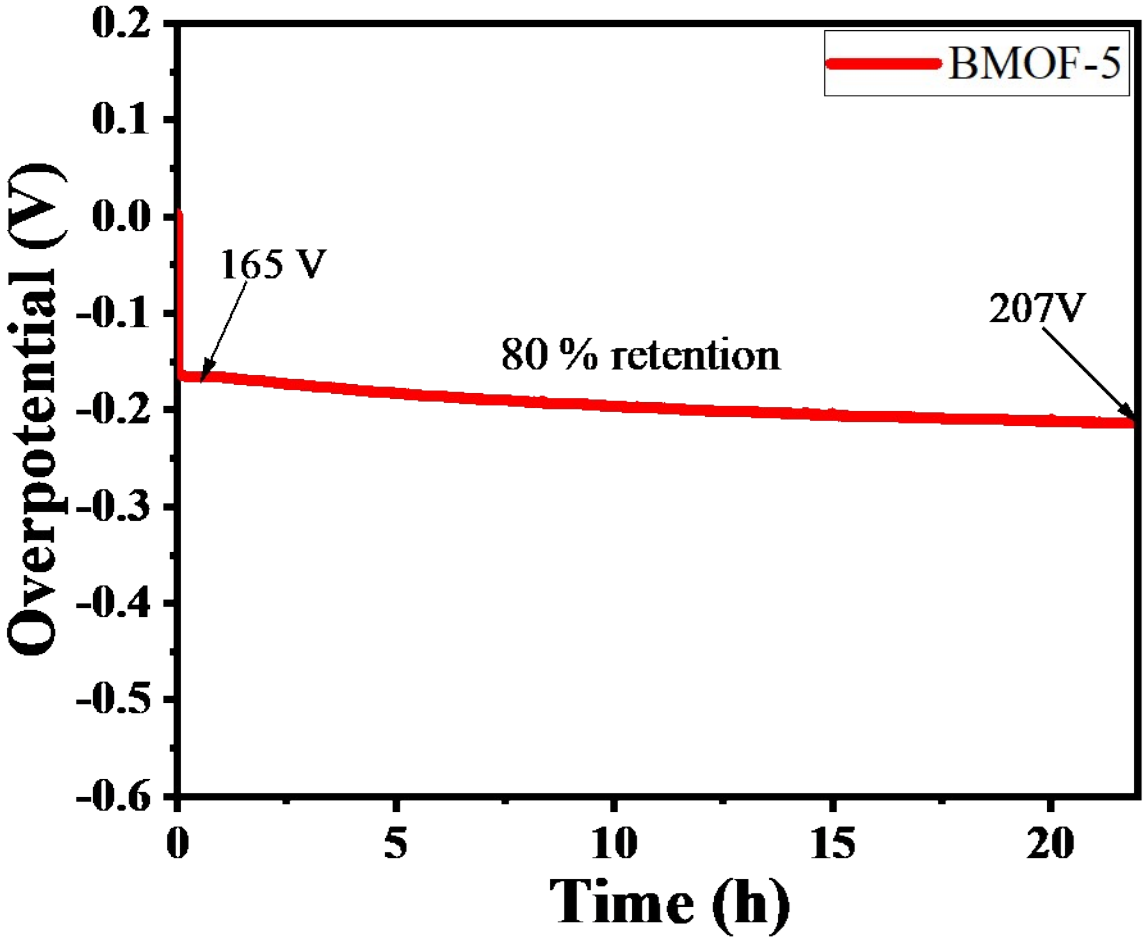


**Figure S15:** Chronopotentiometry test for HER at 10 mA/cm$^2$ current density (without iR correction) for 22 h for the BMOF-5 sample.

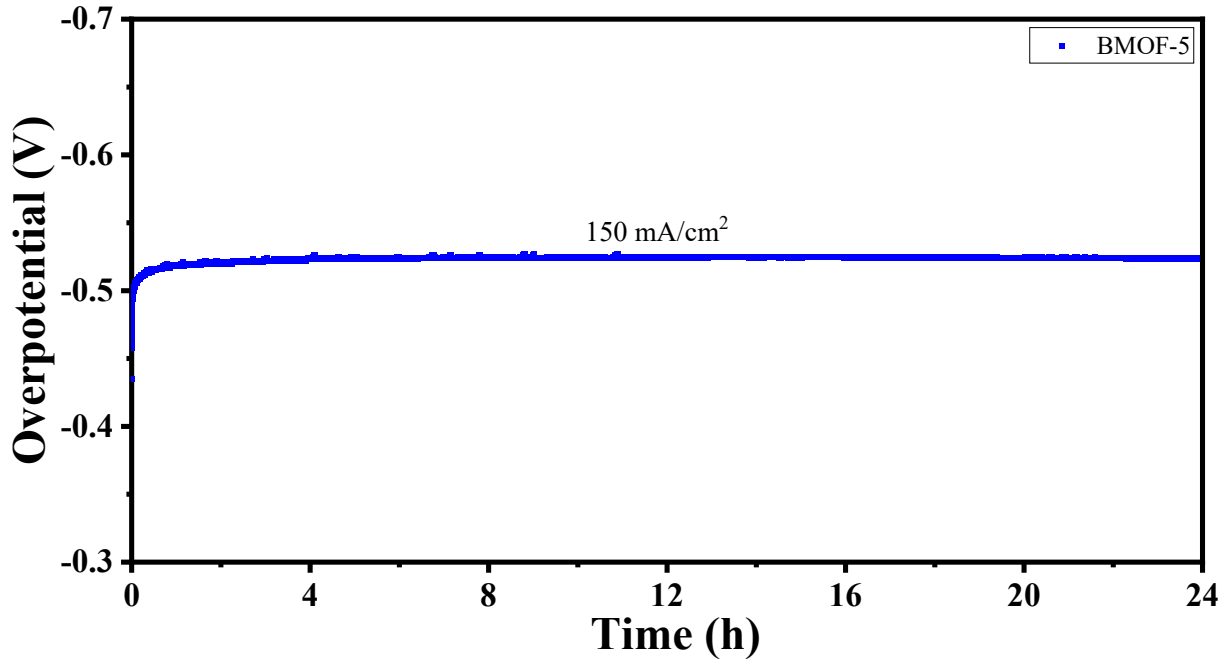


**Figure S16:** Chronopotentiometry test for HER at 150 mA/cm$^2$ current density (without iR correction) for 24 h for the BMOF-5 sample.

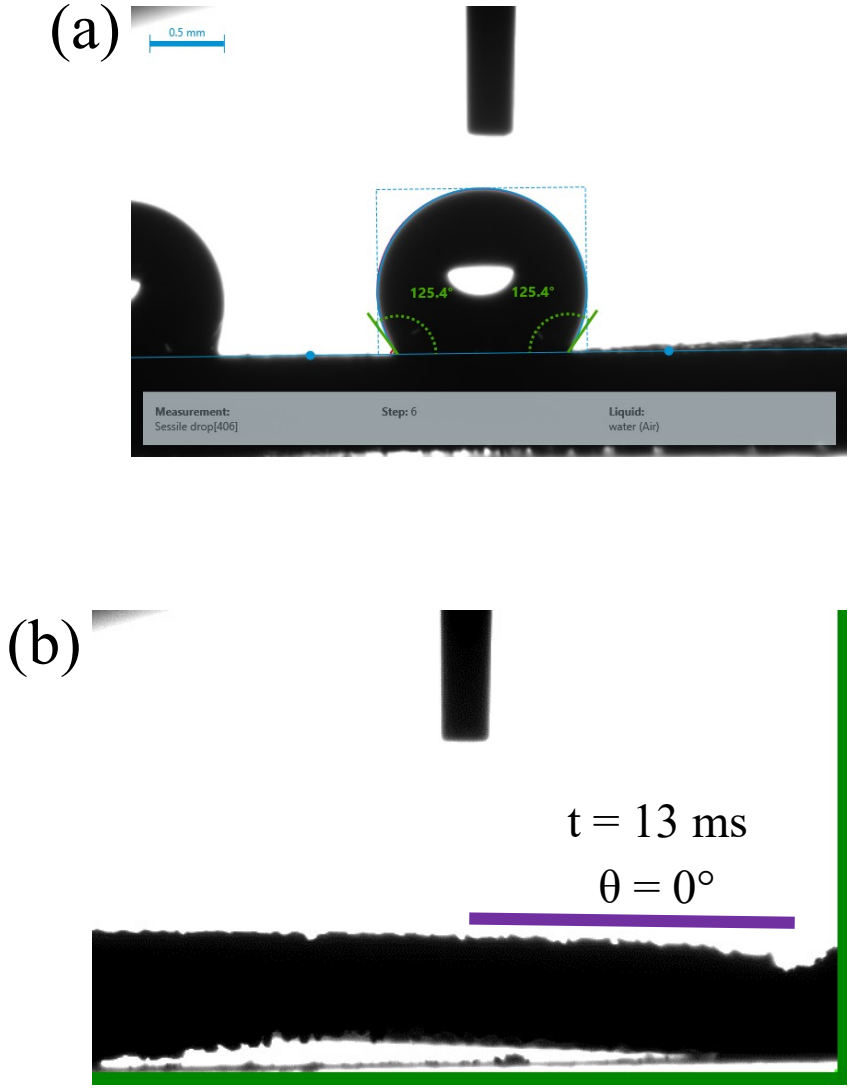


**Figure S17:** Contact angle measurement of Ni-foam and BMO-5 samples, the BMOF-5 shows a superhydrophilic nature.

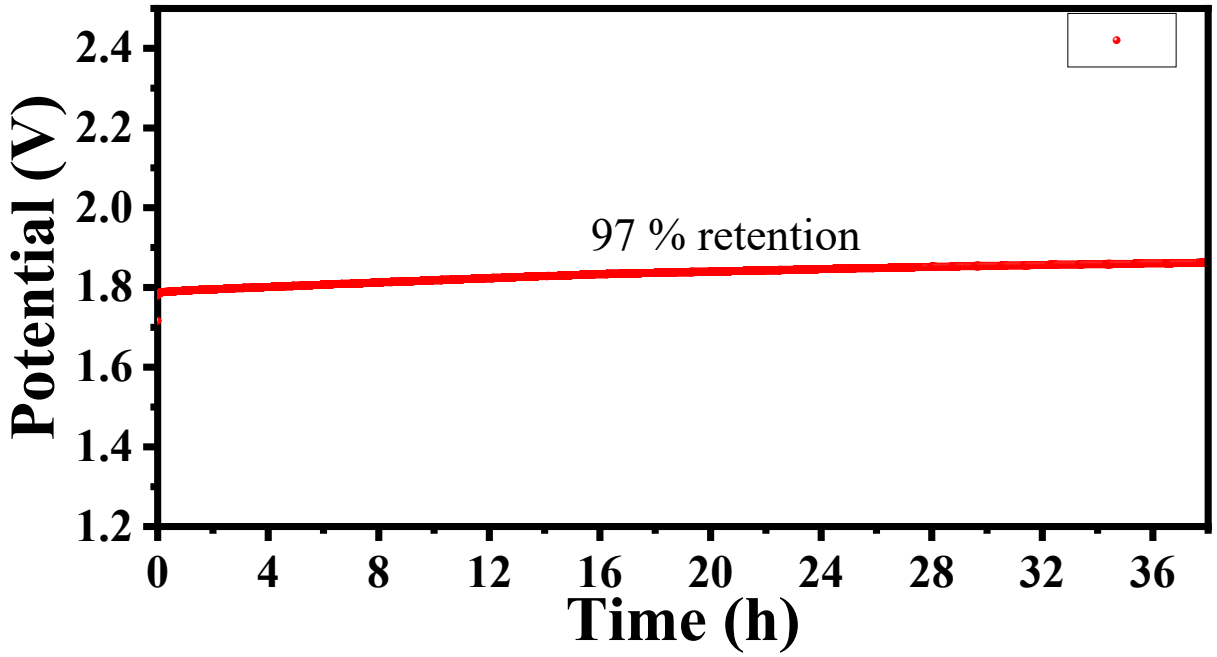


**Figure S18:** Chronopotentiometry test for overall water splitting at 20 mA/cm$^2$ current density (without iR correction).

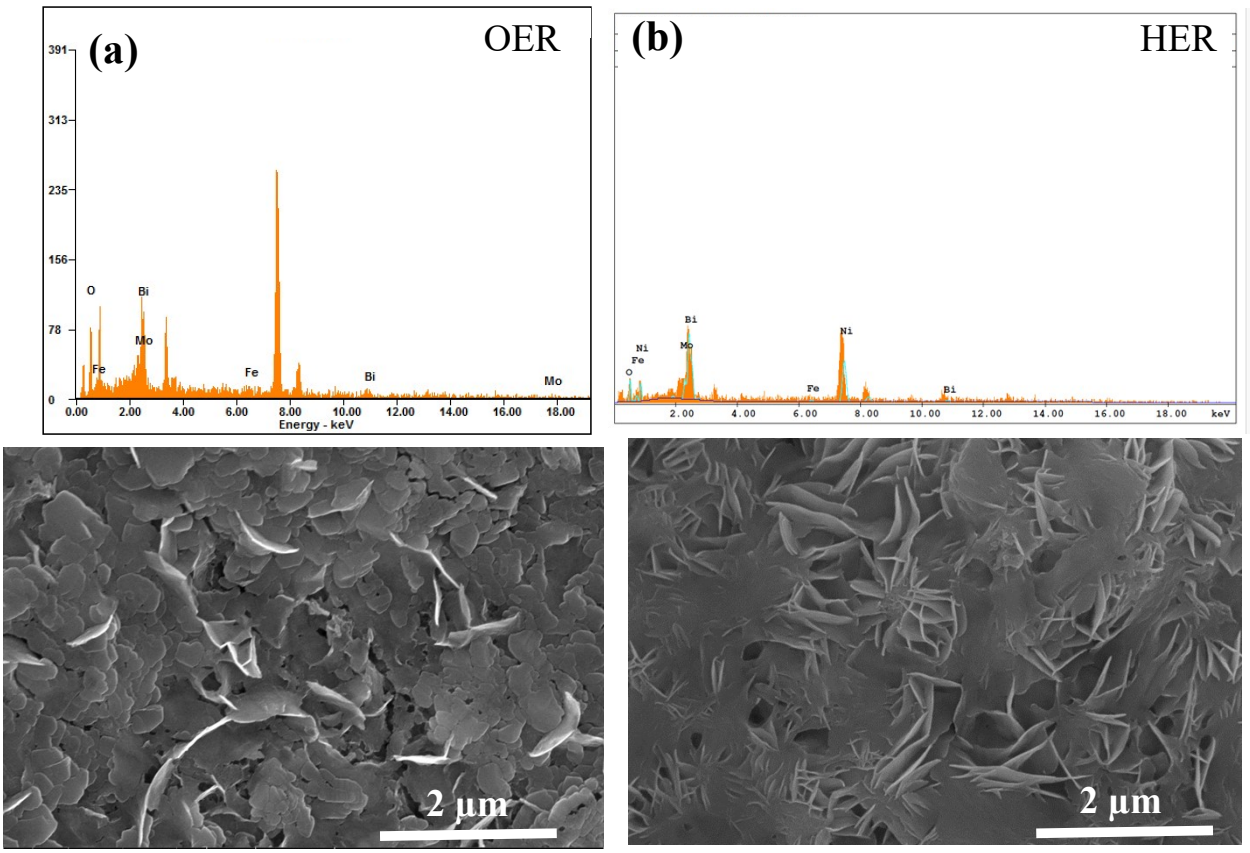


**Figure S19:** (a) EDAX spectrum and FESEM images of the BMOF-5 sample, after electrocatalytic OER, (b) EDAX spectrum and FESEM images of the BMOF-5 sample, after electrocatalytic HER.

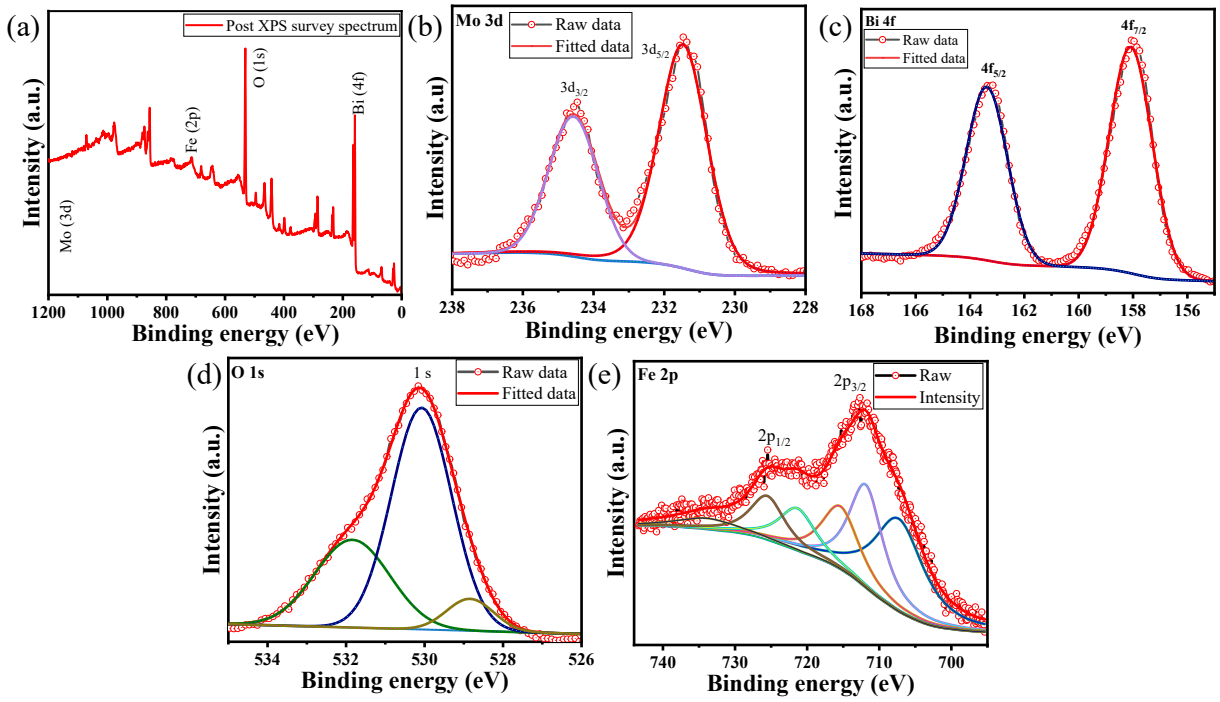


**Figure S20:** Post-catalysis; (a) XPS survey spectrum of BMOF-5, (b) high-resolution XPS spectrum of Mo 3d, (c) high-resolution XPS spectrum of Bi 4f, (d) high-resolution XPS spectrum of O 1s, and (e) high-resolution XPS spectrum of Fe 2p.

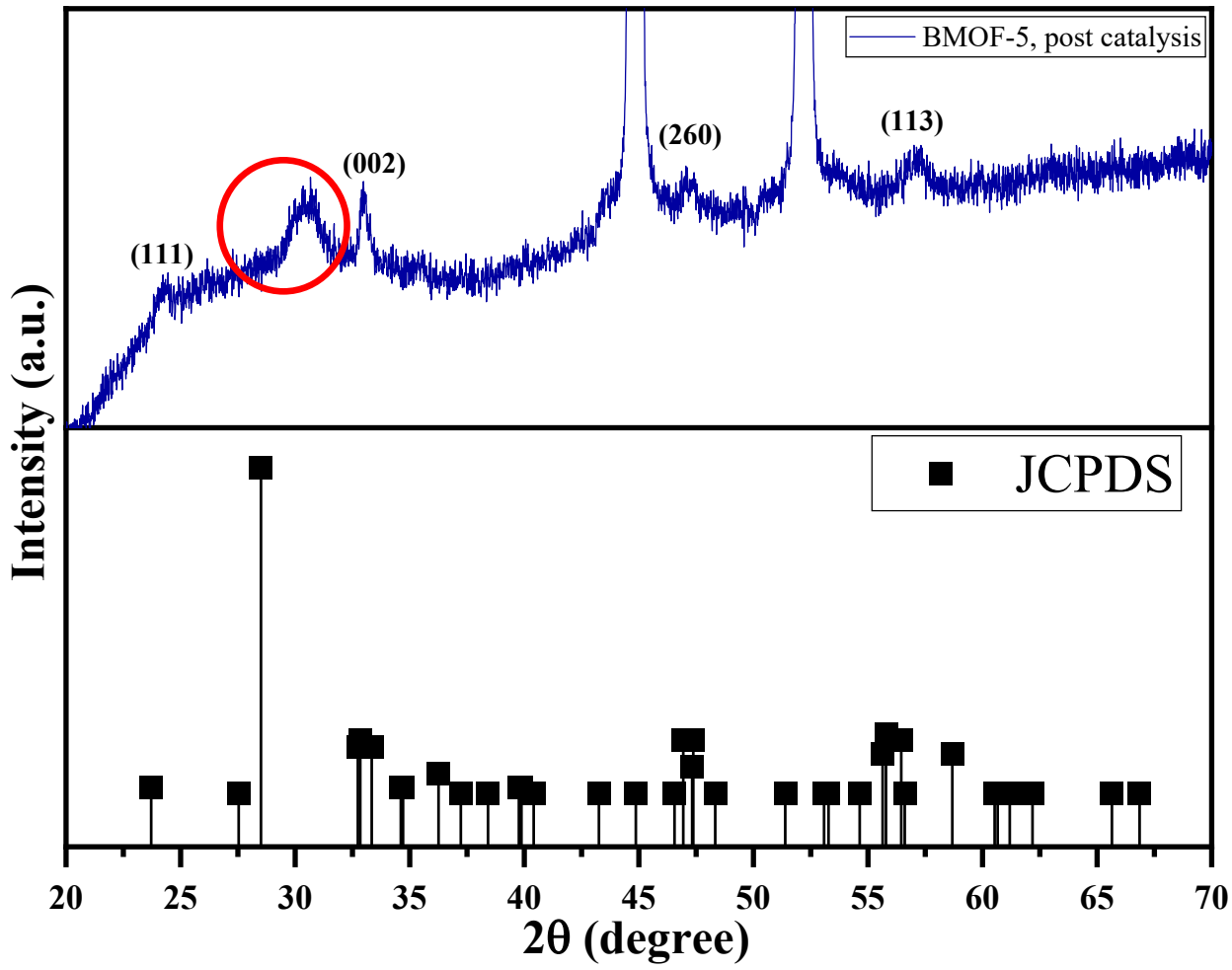


**Figure S21:** Post OER PXRD patterns of BMOF-5 sample after 50h stability test at 20 mA/cm$^2$ current density.